Journal of Sound and Vibration (2002) **250**(2), 323–338
doi:10.1006/jsvi.2001.3934, available online at http://www.idealibrary.com on IDEAL®

COMBINATION OF FINITE AND BOUNDARY ELEMENT METHODS IN INVESTIGATION AND PREDICTION OF LOAD-CONTROLLED NOISE OF POWER TRANSFORMERS

M. Rausch, M. Kaltenbacher, H. Landes and R. Lerch

Department of Sensor Technology, University of Erlangen-Nuremberg, Paul-Gordan-Str. 3-5, *D*-91052 *Erlangen, Germany. E-mail: martin.rausch@lse.e-technik.uni-erlangen.de*

J. Anger and J. Gerth

ABB Transformatoren GmbH., P.O. Box 1580, *D*-53585 *Bad Honnef, Germany*

and

P. Boss

ABB Sécheron SA., P.O. Box 2095, *CH*-1211 *Genéva* 2, *Switzerland*

(*Received* 1 *December* 2000, *and in final form* 16 *July* 2001)

A recently developed calculation scheme for the computer modelling of the load-controlled noise of oil-insulated three-phase power transformers is presented. This modelling scheme allows the precise and efficient computation of the coupled electromagnetic, mechanical and acoustic fields. The equations are solved using the finite element method (FEM) as well as the boundary element method (BEM), resulting in a separation of the calculation of the winding and tank surface vibrations (using FEM) and the computation of the acoustic free-field radiation (using BEM). The complex dynamic behaviour of the loaded transformer can then be studied and, furthermore, an appropriate computer-aided design including an investigation and optimization of design parameters can be established.

The validity of the computer simulations has been verified by means of appropriate measurements. Simulated and measured values for winding and tank surface vibrations as well as sound power levels of the loaded transformer are found to be in good agreement. The applicability of the calculation scheme with respect to the computer-aided design of power transformers is demonstrated by reporting two practical applications: the influence of the stiffness of winding supports and the influence of the tap changer positions.

1. INTRODUCTION

The sound emission of power transformers conflicts more and more with stricter low emission standards, which must be fulfilled, especially at night. Therefore, the prediction and reduction of these sound emissions is of increasing interest for the electrical power industry.

The transformer noise is mainly caused by the following sources [1, 2]: (1) the no-load noise caused by magnetostrictive strain of core laminations; (2) the noise produced by fans or oil pumps; and (3) the *load-controlled noise* caused by Lorentz forces resulting from the interaction between the magnetic stray field of one current-carrying winding and the total

0022-460X/02/070323 + 16 $35.00/0

electric currents in the conductors of the other winding. These forces cause vibrations of the windings and result in acoustic radiations with twice the line frequency (100 or 120 Hz).

In recent decades, the magnetic noise caused by magnetostrictive strain of the core laminations and the noise of fans have been investigated and reduced considerably [3–5]. Due to these improvements, the coil-emitted noise has become of increasing interest and, therefore, has recently been the subject of investigations [6]. At present, approximate empirical prediction formulae, which primarily depend only on the rated power of the transformer, represent the state of the art. However, the main disadvantage of these prediction formulae is that accurate parameters on the load-controlled noise are not available. Since experimental-based investigation of the coil-emitted noise is a lengthy and costly process, the need for appropriate numerical simulation tools arises.

So far, neither finite element methods (FEM) nor boundary element methods (BEM) have been effectively utilized in the prediction and investigation of the load-controlled noise of power transformers. Therefore, most transformer manufacturers still rely on the empirical prediction formulae. The main reason for the lack of computer simulations based on FEM and BEM is the complex interaction of different design parameters and the coupled physical fields. Since, in the case of oil-insulated power transformers, the interaction with the surrounding oil within the tank must not be neglected, the loaded transformer represents a typical magnetomechanical system immersed in an acoustic fluid. That is why, for the precise calculation of the load-controlled noise, the electromagnetic field, the mechanical displacement field, as well as the acoustic pressure field, including their couplings, have to be considered as one system that cannot be separated. Due to the complexity of this multi-field problem, the straightforward application of standard simulation tools suffers from problems of great inefficiency and has shown only limited success.

Therefore, the following steps have been taken into account for these points and, thus, to overcome some of the shortcomings of commercially available general purpose FEM–BEM packages.

- Special so-called magnetomechanical finite elements allow the simultaneous solution of magnetic and mechanical systems and take account of their strong mutual coupling [7].
- Furthermore, a recently developed modelling scheme for a voltage-loaded moving coil enables the coupled system to be treated in a single calculation step [8]. These special so-called magnetomechanical coil elements differ from the standard iterative coupling scheme, where magnetic and mechanical systems are iterated until equilibrium of the whole system is reached.
- Furthermore, in order to consider exactly the feedback between the magnetomechanical device and the surrounding acoustic fluid, acoustic finite elements solve the general linear wave equation governing the propagation of acoustic waves in the ambient fluid and ensure the coupling between the mechanical and acoustic quantities [9].
- Finally, due to sophisticated algorithms and data structures, all matrices as well as auxiliary data are kept in the computer's memory. Therefore, no additional disk space is needed and time-consuming data transfer is reduced to a minimum

This calculation scheme has been implemented in the finite element/boundary element program CAPA [10], which is used here for modelling the dynamic behaviour of power transformers.

In the following, the theory of coupled magnetomechanical–acoustic systems is first reviewed and the corresponding combined finite element and boundary element models are described. Next, comparisons between simulation results and corresponding measured data are shown for verification purposes. Finally, the application of computer simulation studies are presented which investigate the influence of the stiffness of winding supports and tap changer position on the winding and tank surface vibrations as well as on the surrounding sound pressure levels.

2. GOVERNING EQUATIONS

For the computer simulation of the load-controlled noise of oil-insulated power transformers, the following physical fields have to be modelled.

2.1. MAGNETIC FIELD

The governing equation describing the magnetic part of magnetomechanical systems can be derived from Maxwell's equations. Due to the solenoid magnetic field, the magnetic flux density $\mathbf{B}$ can be expressed as the curl of the magnetic vector potential $\mathbf{A}$

$$\mathbf{B} = \nabla \times \mathbf{A}. \tag{1}$$

In the case of low frequencies (neglecting displacement current), the magnetic field is described by the partial differential equation [11]

$$\nabla \times \left(\frac{1}{\mu} \nabla \times \mathbf{A} \right) = \mathbf{J}_e - \gamma \frac{\partial \mathbf{A}}{\partial t} - \gamma \nabla V, \tag{2}$$

where $\mathbf{J}_e$ denotes the free current density, μ the permeability, V the scalar electric potential and γ the electrical conductivity. The second term of the right-hand side of equation (2) represents the induced eddy current density in an electrically conductive body at rest, which is placed in a time-varying magnetic field. The third term of equation (2) expresses the current density due to the potential difference in a conductor.

2.2. MECHANICAL FIELD IN A SOLID

In the case of linear elasticity and isotropic material data, the dynamic behaviour of mechanical systems can be described by the following partial differential equation [12]:

$$\frac{E}{2(1+\nu)} \left((\nabla \cdot \nabla)\mathbf{d} + \frac{1}{1-2\nu} \nabla(\nabla \cdot \mathbf{d}) \right) + \mathbf{f}_V = \rho \frac{\partial^2 \mathbf{d}}{\partial t^2}. \tag{3}$$

In equation (3), E denotes the modulus of elasticity ν, the Poisson ratio, ρ the density, $\mathbf{f}_V$ the volume force and $\mathbf{d}$ the mechanical displacement.

2.3. ACOUSTIC FIELD IN A FLUID

The propagation of an acoustic wave in a homogeneous non-viscous fluid medium is governed by the linear wave equation [13]

$$\nabla^2 p = \frac{1}{c^2} \frac{\partial^2 p}{\partial t^2}, \tag{4}$$

where p is the acoustic pressure and c the sound velocity in the fluid. The scalar velocity potential ψ, given by

$$p = \rho \frac{\partial \psi}{\partial t}, \tag{5}$$

with ρ denoting the density of the fluid, obviously satisfies the same equation

$$\nabla^2 \psi = \frac{1}{c^2} \frac{\partial^2 \psi}{\partial t^2}. \tag{6}$$

In order to obtain a full description of the dynamic behaviour of a loaded power transformer, all coupling terms between the three physical fields have to be considered (see sections 2.4 and 2.5).

2.4. COUPLING "MAGNETIC FIELD – MECHANICAL FIELD"

In the case of a moving conductor in a magnetic field, the term

$$\gamma \mathbf{v} \times (\nabla \times \mathbf{A}) \tag{7}$$

has to be added to equation (2). This term represents the induced eddy current density in an electrically conductive body moving with velocity $\mathbf{v}$ in a magnetic field (motional emf). Here, the velocity $\mathbf{v}$ is given as the time derivative of the mechanical displacement $\mathbf{d}$:

$$\mathbf{v} = \frac{\partial \mathbf{d}}{\partial t}. \tag{8}$$

However, in the case of loaded power transformers, the main coupling between the mechanical and the magnetic field is due to the magnetic volume force $\mathbf{f}_V$ resulting from the interaction between the magnetic stray field of a current-carrying winding and the total electric currents in the other winding. These Lorentz forces, which are proportional to the squared electric current, cause the vibrations of the windings and result in acoustic radiations with twice the line frequency (100 or 120 Hz). This volume force can be computed by

$$\mathbf{f}_V = \mathbf{J} \times \mathbf{B} = \left(\mathbf{J}_e - \gamma \frac{\partial \mathbf{A}}{\partial t} - \gamma \nabla V + \gamma \mathbf{v} \times (\nabla \times \mathbf{A}) \right) \times (\nabla \times \mathbf{A}), \tag{9}$$

where $\mathbf{J}$ denotes the total electric current density.

2.5. FLUID–SOLID INTERACTION

In the case of a fluid–solid interaction, continuity requires that the normal component of the particle velocity $\partial \psi / \partial n$ of the fluid must equal the normal component of the surface velocity v_n of the solid at the interface. Thus, the following coupling condition at a fluid–solid interface is derived:

$$v_n = \mathbf{n} \cdot \left(\frac{\partial \mathbf{d}}{\partial t} \right) = -\, \mathbf{n} \cdot \nabla \psi = -\frac{\partial \psi}{\partial n}. \tag{10}$$

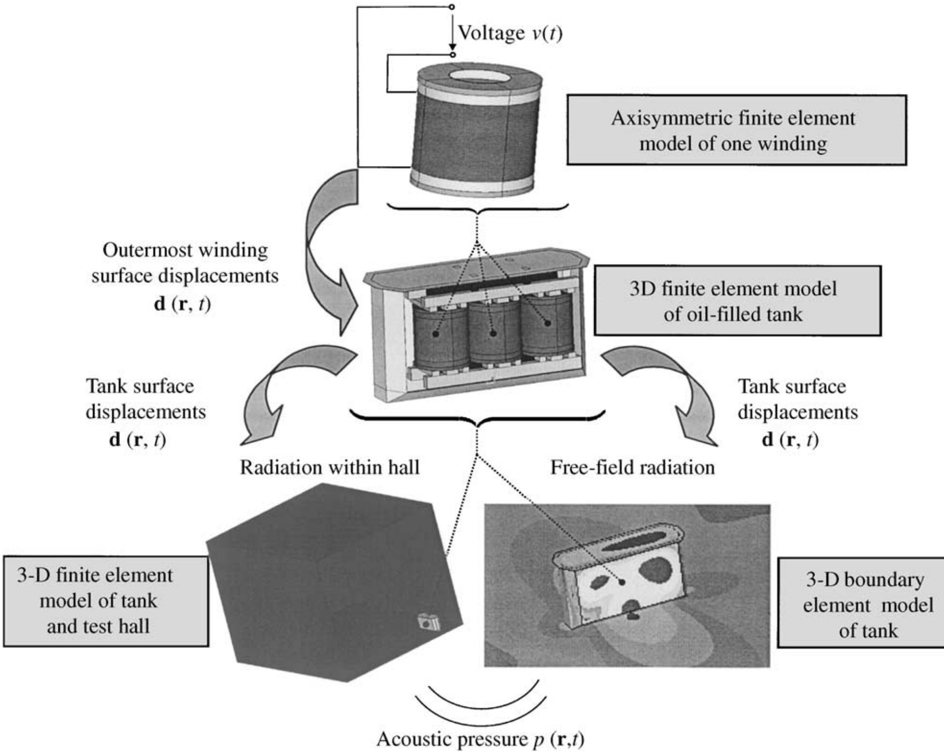

Figure 1. Overview of the calculation scheme.

3. COMBINED FINITE ELEMENT AND BOUNDARY ELEMENT MODELS

3.1. OVERVIEW

In this paper, the governing equations are solved using the finite element method (FEM) as well as the boundary element method (BEM). Thereby, a separation of the computation of the winding and tank surface accelerations (using FEM) and the calculation of the acoustic free-field radiation (using BEM) can be achieved (see Figure 1). Furthermore, for verification purposes, the acoustic radiation within a high-voltage laboratory has been modelled using a three-dimensional acoustic–mechanical finite element model.

The theory of the underlying finite element and boundary element scheme has already been reported in references [7, 8, 14] and will not be repeated here. Meanwhile, the scheme of the voltage-loaded moving coil reported in reference [8] has been updated by a more efficient approach [15]. Since each winding of the coil must carry the same current I, this also has to be ensured for each finite element. Therefore, when a large number of finite elements is required for the discretization of the coil domain, the amount of non-zero entries in the coupling matrix increases resulting in a poor band structure of the overall system matrix. To overcome this shortcoming, the advanced coil-modelling scheme reported in reference [15] enables a decoupling of the defining equations for the magnetic vector potential and the current. Furthermore, the resulting system of equations now contains only the effective mass matrix of the magnetic system instead of the overall system matrix [15]. The required computer resources are thereby reduced tremendously (see section 3.2).

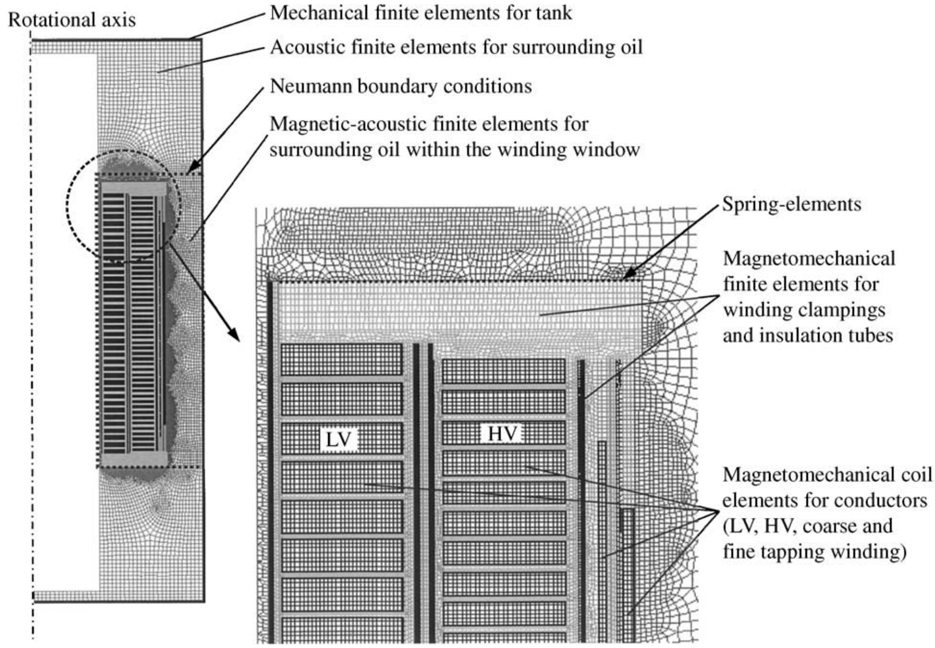

Figure 2. Axisymmetric acoustic–magnetomechanical finite element model of one winding of the oil-filled power transformer.

3.2. MODELLING OF THE WINDING VIBRATIONS

The first step in the modelling scheme calculates the outermost winding surface displacements by an acoustic–magnetomechanical finite element model of one winding of the oil-filled transformer. Due to rotational symmetry of the windings and symmetric load (as a result of the ideal measurement condition in the factory test field), a two-dimensional (2D) finite element model based on axisymmetric elements can be used (see Figure 2). In the finite element model, the voltage-loaded conductors of the windings are discretized using the so-called magnetomechanical coil elements. These elements solve the equations governing the electric circuit, the magnetic as well as the mechanical field quantities, and take account of the full coupling between these fields (see section 2). All winding clamping and insulation materials between each coil as well as the winding support platforms are modelled using magnetomechanical finite elements, which solve the coupled magnetic and mechanical field quantities. Instead of a complete model of the highly permeable core by magnetic finite elements, this computer model was simplified by applying *Neumann* boundary conditions at the border of the winding window (see Figure 2). Furthermore, the surrounding oil within the tank is discretized using pure acoustic finite elements and magnetic–acoustic finite elements (solving the magnetic as well as the acoustic partial differential equation without any coupling). Finally, the tank is modelled using standard mechanical finite elements.

Additionally, the following aspects have to be considered for the precise computer simulation of the winding vibrations of loaded power transformers.

(1) To measure the load-controlled noise in a factory test field, the transformer has to be operated at short circuit and at rated currents. In this case, due to the small voltage during the short-circuit test, the core-emitted noise can be neglected and, therefore,

a clear distinction between the no-load noise and the load-controlled noise can be achieved. In the simulations, this effect was taken into account by modelling the innermost low-voltage (LV) winding as a voltage-loaded coil with an external voltage of zero. The high-voltage (HV) winding and both in-series connected, outermost tapping windings, however, are loaded with the measured short-circuit voltage in “star connection”.

(2) Furthermore, the core clamping supports have been ignored in the finite element model to reduce the effort. Therefore, the influence of these supports, which consists of an additional axial stiffness of the winding, is realized by so-called spring elements. As shown in Figure 2, these spring elements have been located at the outside boundary of the upper and lower winding support platform. In the simulations a stiffness of 85 MN/m has been used, which is in accordance with the experience of the transformer manufacturers.

(3) Finally, since measurement results revealed a large influence of the tap changer position on the measured vibrations and sound pressure levels, the following simulations have been performed for three nominal positions.

- *Tap changer position* 1. The HV winding and both tapping windings are connected in-series.
- *Tap changer position* 2. The HV winding and the coarse tapping winding are connected in-series.
- *Tap changer position* 3. Only the HV winding is connected.

For the computation of the amplitude of the winding surface displacements, a dynamic analysis using a sinusoidal 50 Hz (or 60 Hz) excitation signal for the voltage between the two supply terminals of the high-voltage windings was performed. It should be noted that further input parameters are the geometry of the power transformer, the density, modulus of elasticity, the Poisson ratio and loss factor for the mechanical materials (tank, conductors, insulation and clamping materials), the electrical conductivity for the conductors as well as the density and bulk modulus for the surrounding oil. After the computation of the response signals (current in the conductors of both windings as well as mechanical displacements of the outermost winding), the Fourier transform of the output signals has to be calculated. Finally, the 100 Hz (or 120 Hz) component of the spectrum must be extracted.

In the computer simulations 60 000 first order finite elements have been used, resulting in a total number of about 200 000 unknowns. On an SGI, Octane R12000-300 MHz computer, a transient analysis with 1200 time steps required 18 h of CPU time and 1 GByte of physical memory. Using the conventional coil-modelling scheme reported in reference [8], the same computations required 3.2 GByte of physical memory and 58 h of CPU-time.

3.3. MODELLING THE OIL-FILLED TANK

In the second step in the developed calculation scheme, the previously calculated winding surface displacements are now taken as mechanical excitation in a three-dimensional acoustic–mechanical finite element model of the complete oil-filled tank (see Figure 3). Furthermore, in the three-dimensional finite element model, the 120° phase shift between the three windings is taken into account.

In this model the tank, the core clampings, as well as the connections between core clampings and the top of the tank, are modelled using mechanical finite elements. Furthermore, the surrounding oil within the tank is discretized using acoustic finite elements. Finally, the additional stiffness of the core clamping supports is again

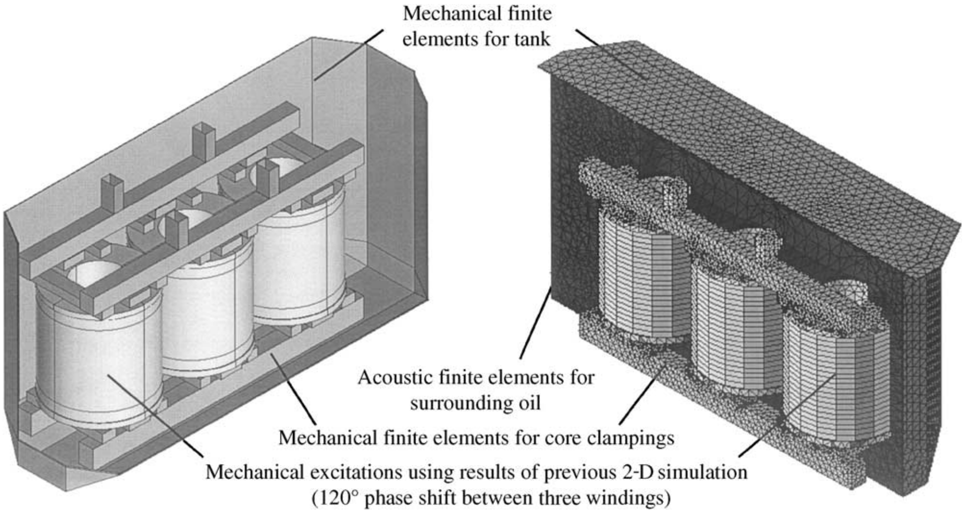

Figure 3. Three-dimensional acoustic–mechanical finite element model of an oil-filled transformer.

implemented using spring elements. Because the load-controlled noise is primarily a simple 100 Hz (or 120 Hz) tone, a harmonic analysis for this single frequency has been performed in these simulations. The finite element model consisted of 210 000 three-dimensional finite elements, resulting in a total number of about 93 000 unknowns. On an SGI, Octane R12000–300 MHz computer, the in-core solution for the single frequency simulation took 14 h of overall CPU-time and 3.7 GByte of physical memory.

3.4. MODELLING OF THE RADIATED SOUND FIELD

In the final step, the previously calculated tank surface vibrations are now applied as mechanical excitation in the final acoustic simulations to calculate the radiated transformer noise. Here, the free-field radiation and the radiation within closed rooms such as a high-voltage laboratory are calculated (see Figure 1).

For the computation of the free-field sound radiation, the complete structure of the tank has been discretized using boundary elements (see Figure 4). Due to the fact that the coil-emitted noise is primarily a simple 100 Hz (or 120 Hz) tone and that the vibrating air surrounding the transformer does not react on the tank vibrations, a boundary element method is well suited for predicting transformer noise radiation from acceleration data. Furthermore, in these simulations the transformer was assumed to be positioned on an ideal reflecting ground, so that a half-space boundary condition could be applied. The model consisted of 3300 boundary elements and the calculation of a single frequency simulation took 40 min of overall CPU-time and 160 MByte of physical memory on an SGI, Octane R12000–300 MHz computer.

On the other hand, for the computation of the sound radiation within a high-voltage laboratory, a three-dimensional acoustic–mechanical finite element model has been set up (see Figure 5). Here, the tank of the transformer is discretized using mechanical finite elements. Furthermore, the surrounding air within the test hall is modelled using acoustic finite elements. The walls of a typical high-voltage laboratory are not covered with any absorbing material. Therefore, in these simulations the transformer was assumed to be positioned within a room with ideal reflecting walls. In this computer simulation, 640 000

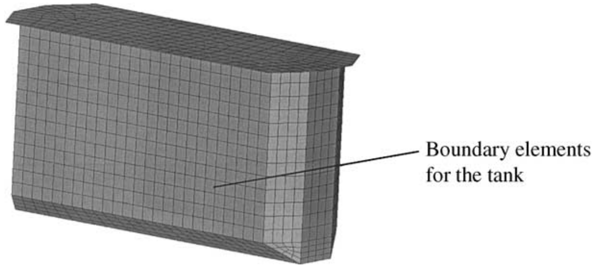

Figure 4. Three-dimensional (3-D) boundary element model of the transformer tank.

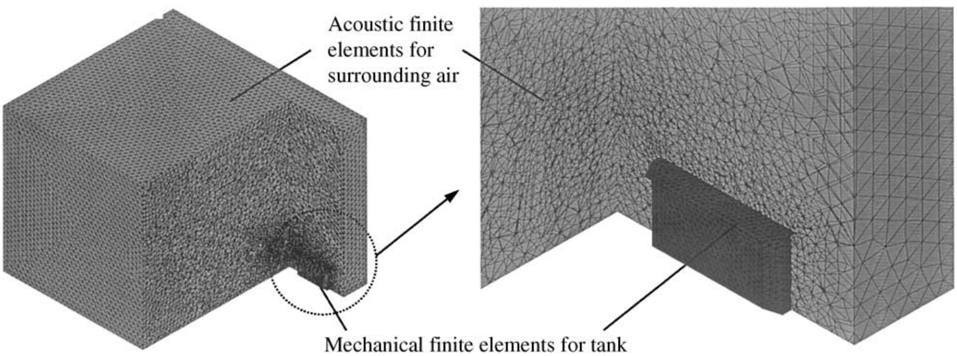

Figure 5. Three-dimensional acoustic–mechanical finite element model of the transformer tank and the high-voltage laboratory.

three-dimensional finite elements have been used. The resulting system of equations had a total number of 115 000 unknowns and the harmonic calculation of a single frequency simulation took 9 h of overall CPU-time and 3·5 GByte of physical memory on an SGI, Octane R12000–3000 MHz computer.

4. VERIFICATION OF THE COMPUTER MODELS

The verification of the computer models described above has been performed by comparing simulation results with corresponding measured data. It should be noted that due to the complexity of the sound emission of the loaded power transformer, analytic calculations are unavailable and, therefore, cannot be used for verification purposes.

4.1. VERIFICATION OF THE CALCULATED WINDING AND TANK SURFACE VIBRATIONS

In a first step, the axisymmetric finite element model has been verified by comparing measured and calculated short-circuit currents, mechanical eigenfrequencies as well as winding surface accelerations.

In Table 1, the short-circuit currents obtained by measurements as well as simulations are shown for two tap changer positions. The good agreement between measured and calculated values (deviation is within 1·25%) validates again the developed coil-modelling scheme.

TABLE 1

Measured and simulated short-circuit currents

	Measurement (A)	Simulation (A)
Current in LV winding at tap changer position 1	825	832
Current in HV winding at tap changer position 1	159	161
Current in LV winding at tap changer position 2	825	825
Current in HV winding at tap changer position 2	180	181

Note: LV, low-voltage; HV, high-voltage.

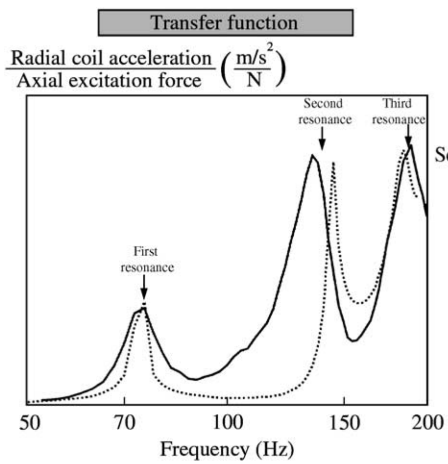

Mechanical eigenfrequencies

	Measured	Simulated
First resonance	75 Hz	75 Hz
Second resonance	135 Hz	145 Hz
Third resonance	190 Hz	188 Hz

Figure 6. Comparison of measured and simulated transfer functions and mechanical eigenfrequencies of the winding mounted on the core: ——, measurement with piezoelectric accelerometer; ⋯⋯, finite element simulation.

Next, the measured and calculated transfer functions and mechanical eigenfrequencies of the complete winding system mounted on the core have been compared (see Figure 6). The deviation at the second eigenfrequency is due to the fact that the actual winding does not show an exact axisymmetric construction. Furthermore, it should be noted that the winding was axially excited at the upper winding support platform and the resulting radial coil acceleration of the outermost winding was measured as well as simulated.

In a final verification of the axisymmetric finite element model, the simulation results have been compared with corresponding measured winding surface accelerations. Here, the axial accelerations on the upper winding support platform and the radial vibrations on the outermost fine tapping winding were measured using an oil-resistant piezoelectric accelerometer. The measurements showed that the sensitivity of these sensors against electromagnetic interferences of the high-voltage windings is negligible. Furthermore, the derivations of subsequent measurements were within a range of $\pm 1{\cdot}5\%$. In Table 2, the winding vibrations of the transformer without tank, and in Table 3 the normalized accelerations of the transformer with oil-filled tank are compared respectively. In the case of the transformer with an oil-filled tank (see Table 3), measurements as well as simulations reveal that the surrounding oil does not influence the axial accelerations of the winding support platform. However, due to the mass-loading effect of the surrounding oil, the radial coil acceleration amplitudes are nearly halved when compared to the vibrations ignoring

TABLE 2

Transformer without oil-filled tank: measured and simulated winding accelerations

	Measurement (m/s^2)	Simulation (m/s^2)
Radial coil acceleration at tap changer position 1	0·047	0·046
Axial clamping acceleration at tap changer position 1	0·036	0·037
Radial coil acceleration at tap changer position 2	0·021	0·019
Axial clamping acceleration at tap changer position 2	0·031	0·032

TABLE 3

Transformer with oil-filled tank: measured and simulated winding accelerations

	Measurement†	Simulation†
Radial coil acceleration at tap changer position 1	0·59	0·62
Axial clamping acceleration at tap changer position 1	0·96	0·99

†Normalized to the corresponding result without an oil-filled tank (see Table 2).

TABLE 4

Measured and simulated tank accelerations

Position	Measurement (m/s^2)	Simulation (m/s^2)
1	0·16	0·13
2	0·063	0·075
3	0·14	0·1
4	0·055	0·07
5	0·04	0·05
6	0·029	0·03
7	0·01	0·015
8	0·02	0·025
9	0·04	0·045

the oil-filled tank. In summary, it can be stated that an axisymmetric finite element model predicts the winding surface accelerations of a loaded power transformer precisely for both configurations, with and without an oil-filled tank (see Tables 2 and 3).

Finally, the three-dimensional acoustic–mechanical finite element model of the oil-filled tank has been verified by comparing the calculated tank side wall accelerations with values measured at nine different positions (see Table 4).

4.2. VERIFICATION OF THE SOUND FIELD CALCULATIONS

After these basic validations of the computational models, the A-weighted sound power level of the short-circuited transformer was measured in accordance with the European

TABLE 5

Radiation within closed rooms: measured, simulated and predicted sound power levels

	Sound power level (dB(A))
Sound pressure measurement according to reference [16]	68
Finite element simulation	66·5
Empirical prediction formula according to reference [16]	63·5
Empirical prediction formula according to reference [16]	60·5

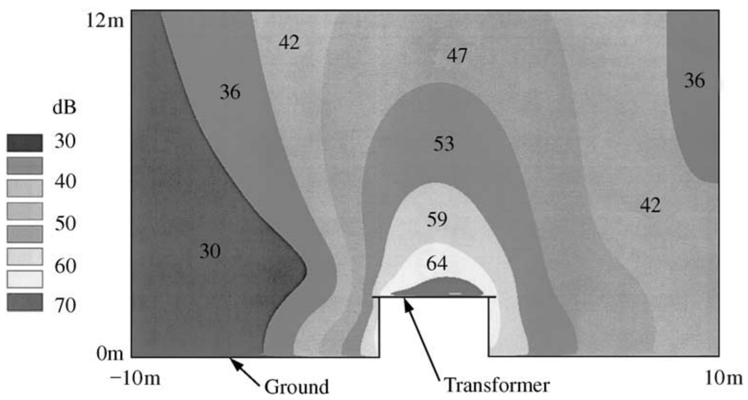

Figure 7. Freefield radiation: sound pressure levels along the longitudinal plane of symmetry of the transformer calculated by the boundary element analysis.

standard EN 60551 [16] and compared with the corresponding acoustic simulations. This standard requires that the A-weighted sound pressure levels around the transformer have to be measured at a distance of 0·3 m from the tank surface and at half the tank height. Furthermore, these measurements have to be performed in a typical high-voltage laboratory at the premises of a transformer manufacturer. Due to this fact, the first step in this verification procedure used the three-dimensional finite element model already used for the calculation of the radiated noise within closed rooms, as shown in Figure 5. An A-weighted sound power level of 66·5 dB was calculated from the simulated sound pressure levels. Considering that the reproducibility of the sound pressure measurements lies within a range of ± 1 dB, a good agreement between measurement and simulation was achieved (see Table 5).

Furthermore, as can be seen from Table 5, in this case the deviations between measured and calculated sound power level are considerably smaller than those resulting from the current prediction formulae for the load-controlled noise. Therefore, it can be concluded that this pure finite element scheme is well suited to the computation of the load-controlled noise of oil-filled power transformers, which are operated within a typical high-voltage laboratory.

After the verification of the sound field calculation within closed rooms, the half-space free-field sound radiation of the transformer has been calculated using the boundary element model, as depicted in Figure 4. The calculated sound pressure levels along the longitudinal plane of symmetry of the transformer are shown in Figure 7.

TABLE 6

Freefield radiation: measured, simulated sound power levels

	Sound power level (dB(*A*))
Sound pressure measurement according to reference [16]	68
Sound intensity measurement according to reference [17]	61
Boundary element simulation	59

This three-dimensional sound field calculation reveals two important effects, which are of great interest for transformer manufacturers:

- First, the sound power level calculated by the boundary element analysis results in an A-weighted sound power level of only 9 dB, which is about 7 dB lower than the level obtained by the previous finite element simulation (see Table 5). Therefore, the result of the boundary element simulation indicates a problem with the sound pressure measurements, which were made according to the current transformer noise measurement standard EN 60551. In the case of load-controlled noise (low-frequency noise of 100 Hz), sound pressure measurements at a distance of 0·3 m from the tank surface will be in the near field of the transformer and, therefore, may result in a significant overestimation of the sound power level. To reduce the influence of the reactive near field, a sound intensity measurement for the determination of transformer sound power levels is proposed [17]. In order to verify the calculated free-field radiation obtained by the boundary element model, measurements with a sound intensity measuring system have been performed. In Table 6, the measurements using the two methods are compared with the boundary element simulation. As noted before, the sound pressure measurement in accordance to reference [16] gives considerably higher results. The sound intensity measurements result in about 7 dB lower sound power levels and, therefore, confirm the validity of the boundary element model. Therefore, it can be concluded that the combined finite element and boundary element scheme is well suited to the computation of the load-controlled noise of oil-filled power transformers under ideal free-field conditions.

  Furthermore, it should be noted that the sound intensity measurement is also included in the current test standard [16] as an option according to an agreement between the transformer manufacturer and the customer. However, the sound pressure measurement is still the most commonly used method. This is the reason why the empirical prediction formulae should still be compared with the results obtained by the sound pressure measurements (see Table 5).
- Second, these simulations reveal that the radiated sound field shows a strong directional behaviour, which is due to the 120° phase shift in the vibrations of the three windings (see Figure 7). This directional behaviour of the transformer can be reversed by changing the phase order of the windings. Therefore, this effect might be used for an efficient abatement of the load-controlled noise disturbance if the residential area is only located in one direction.

5. APPLICATIONS

The applicability of the present calculation scheme with respect to the computer-aided design of power transformers has been proved by the following applications.

TABLE 7

Influence of the tap changer position obtained by simulation

	Tap changer position 1	Tap changer position 3
Radial coil acceleration (m/s^2)	0·033	0·009
Axial winding clamping acceleration (m/s^2)	0·044	0·033
Tank side wall acceleration (m/s^2)	0·025	0·009
A-weighted sound power level (dB(A))	59	45

5.1. INFLUENCE OF TAP CHANGER POSITION

As a first application, the influence of the tap changer position on the winding and tank surface vibrations as well as on the A-weighted sound power level has been investigated. Table 7 shows the simulation results at tap changer position 1 (HV winding and both tapping windings are connected in-series) and at tap changer position 3 (only the HV winding is connected). Simulations as well as measurements reveal that the radial vibrations of the outermost, fine tapping winding are greatly decreased at tap changer position 3 when compared to position 1.

With these simulations, it was found that the radial magnetic volume forces acting on the innermost LV and HV winding are almost independent of the tap changer position. Therefore, this reduction of the radial coil vibrations at tap changer position 3 is based on the non-current-carrying, outermost, fine tapping winding.

On the other hand, simulation results revealed that the axial magnetic volume forces acting on the LV and HV winding are larger at tap changer position 3 when compared to position 1. This is caused by the edge fringing effect and is responsible for the fact that the axial winding clamping vibrations are almost independent of the tap changer position (see Table 7). Furthermore, due to the decrease of the radial surface accelerations of the outermost winding at tap changer position 3, the tank surface vibrations and, hence, the calculated A-weighted sound power level are greatly reduced.

Therefore, in contrast to reference [6], where it is assumed that only axial winding vibrations are responsible for the load-controlled noise, these simulations clearly show that the radial coil vibrations also have a significant influence on the coil-emitted noise.

5.2. INFLUENCE OF STIFFNESS OF WINDING SUPPORTS

In a second application, the influence of the stiffness of the winding and core supports on the load-controlled noise has been investigated. This stiffness has been modelled in the finite element simulations by applying mechanical spring elements, which were located at the outside boundary of the upper and lower winding support platform (see Figure 2). As expected, the simulations reveal that neglecting this axial stiffness causes significantly increased axial clamping accelerations and slightly decreased radial coil accelerations. Therefore, greatly increased sound pressure levels result (see Table 8). These results indicate that this stiffness has a strong influence on the radiated transformer noise effect, which can be used in the optimization of the system.

The above applications clarify the great advantage of computer modelling studies, where a separation of different effects for the different components of the transformer can be

TABLE 8

Influence of stiffness of winding supports obtained by simulation

	Radial coil acceleration (m/s^2)	Axial winding acceleration (m/s^2)	SPL† in 0·3 m (dB)
With stiffness of winding support 85 MN/m	0·046	0·037	56·8
Without stiffness of winding support	0·044	0·62	82·3

†SPL—Sound pressure level.

achieved. Therefore, the influence of the different physical effects and design parameters on the coil-emitted noise can be very usefully extracted and studied in the simulation.

6. CONCLUSIONS

In this paper, a new numerical scheme based on combined finite element and boundary element models for the precise and efficient computer modelling of the load-controlled noise of power transformers has been applied. The validity of the simulation models has been verified by appropriate measurements. The calculated and measured values for short-circuit currents, mechanical eigenfrequencies of the windings as well as winding and tank surface vibrations compare very well. Furthermore, a good agreement between measured and calculated sound radiation is found. The deviation between measured and calculated A-weighted sound power level is only 1·5 dB in this case. The dependency of the sound radiation of power transformers on some parameters was investigated and helpful results were obtained for the transformer manufacturer. Due to the 120° phase shift in the vibrations of the three windings the radiated sound field shows a strong directional behaviour, which might be used for an efficient abatement of the load-controlled noise disturbance. Furthermore, the studies have shown that the radial coil vibrations have a significant influence on the coil-emitted noise, which is in contrast to previous reports.

The presented computer simulations have been shown to be a useful tool in the prediction, investigation and reduction of the load-controlled noise and reconfirm the value of computer-aided design of power transformers. A complete CAE-tool for the computer-aided design of power transformers will be established in the near future on the basis of the existing software.

REFERENCES

1. M. J. HEATHCOTE 1998 *The J&P Transformer Book*. Oxford: Newnes; twelfth edition.
2. W. DIETRICH 1986 *Transformatoren: Stand der Technik und Tendenzen*, Technische Akademie Wuppertal (TAW). Berlin: VDE-Verlag.
3. H. HÜTTNER 1983 *ELIN-Journal* **1/2**, 41–46. Noise and vibration of transformers, their origin and reduction.
4. M. KANOI, Y. HORI, M. MAEJIMA and T. OBATA 1983 *IEEE Transactions on Power Apparatus and Systems* **PAS-102**, 2817–2825. Transformer noise reduction with new sound insulation panel.
5. E. REIPLINGER and H. STELTER 1977 *elektrotechnische zeitschrift* **98**, 224–228. Geräuschprobleme.
6. E. REIPLINGER 1989 *etz* **110**, 106–109. Lastabhängige Transformatorgeräusche.
7. M. KALTENBACHER, H. LANDES and R. LERCH 1997 *IEEE Transactions on Magnetics* **33**, 1646–1649. An efficient calculation scheme for the numerical simulation of coupled magnetomechanical systems.

8. M. Kaltenbacher, M. Rausch, H. Landes and R. Lerch 1999 *COMPEL* **18**, 504–514. Numerical modelling of electrodynamic loudspeakers.
9. H. Lerch 1988 *Proceedings of IEEE Ultrasonics Symposium*, 643–654 Chicago, U.S.A. Finite element analysis of piezoelectric transducers.
10. H. Landes, R. Lerch and M. Kaltenbacher 2000 *CAPA User Manual*, Release 3·4, University of Erlangen.
11. P. S. Silvester and R. L. Ferrari 1996 *Finite Elements for Electrical Engineers*, Vol. 3. Cambridge: Cambridge University Press.
12. F. Ziegler 1991 *Mechanics of Solids and Fluids*. Vienna: Springer-Verlag.
13. G. S. Kino 1987 *Acoustic Waves*: *Devices*, *Imaging*, *and Analog Signal Processing*. Englewood Cliffs, NJ: Prentice-Hall.
14. R. Lerch, M. Kaltenbacher, H. Landes, M. Rausch. P.-C. Eccardt 2000 in *Boundary Elements in Acoustics in Advances in Boundary Elements Series*. (Ing. Otto von Estorff, editor) Southampton, Boston: Computational Mechanics Publication. Combination of finite element and boundary element methods in computational acoustics and coupled field problems of electro-acoustic transducers.
15. M. Rausch, M. Kaltenbacher, H. Landes and R. Lerch 2000 *Proceedings of 9th International IGTE Symposium on Numerical Field Calculation in Electrical Engineering*, 440–445. Numerical computation of the emitted noise of power transformers.
16. *European standard EN* 60551/*A*1 1997 on Determination of transformer and reactor sound levels.
17. R. P. Kendig 1991 *IEEE Transaction on Power Delivery* **6**, 1524–1530. Validation of acoustic intensity measurements for power transformers.